Climate Modeling, Dynamically Speaking

James Walsh, Department of Mathematics, Oberlin College
Richard McGehee, School of Mathematics, University of Minnesota

Is it true the Earth was completely covered by glaciers at one time in its past? Or have glaciers ever discharged into the ocean at tropical latitudes? Are conceptual energy balance models able to shed any light on the possible occurrence of global events such as these?

Mathematics is playing an ever expanding role in the study of climate. One might point to the creation of the Mathematics and Climate Research Network, an NSF funded group that links researchers across the US in efforts to develop the mathematics needed to better understand climate [**10**]. Or one might note that two plenary talks and no fewer than four minisymposia were devoted to issues arising in the mathematical study of climate at a recent SIAM Conference on Applications of Dynamical Systems [**19**].

Techniques from dynamical systems have recently proved successful in the study of climate (to the point of meriting an Op-Ed piece in the New York Times [**7**]). In this article we present an introduction to a dynamics approach to climate modeling as we consider the questions posed above. Along the way we detail but one part of this success story, while emphasizing aspects of the narrative which are appropriate for the undergraduate curriculum.

A homogeneous Earth model

Energy Balance Models (EBM) are conceptual in nature, providing a broad view of the way in which a specified system variable, such as surface temperature, depends upon a few prominent climate components. These models lie on the opposite end of the spectrum from highly sophisticated General Circulation Models (GCM) ([**5**], for example).

One advantage of EBM is the ease with which one can run simulations over long periods of time, as in the study of large scale glacial cycles, relative to GCM. Another is the focus one is able to place on individual factors and their influence on climate, a role assumed in this article by planetary albedo. Drawbacks include possible model sensitivity with regard to parameter values, given that such quantities are often difficult to determine [**16**]. Additionally, fundamental processes such as cloud feedback, the hydrological cycle, and topographic effects are typically not included in EBM [**15**, §9.2.6]. Nonetheless EBM, belying their simplicity, play an important role in the study of climate, as succinctly stated by Gerald North in [**13**]:

> Though the path to understanding global climate is obviously complicated, it is clear that mathematical modeling is the best starting point to test assumptions against geological and present day evidence.

Global climate is determined by the radiation balance of the planet. The Earth warms through the absorption of incoming solar radiation (or *insolation*). Due to the shortwave nature of radiation emitted by the sun, much of this energy passes freely through Earth's atmosphere. The Earth cools by radiating energy back into space, albeit at longer wavelengths, and some of this *Outgoing Longwave Radiation* (OLR) is absorbed by the atmosphere [**15**, chapter 3]. Though we will derive an equation shortly for the surface temperature via energy balance, this balance actually occurs at the top of the atmosphere (the level of the atmosphere at which radiation is emitted back into space, roughly 5 km above the surface). EBM therefore do not explicitly include terms corresponding to the complicated and myriad transfers of energy within the atmosphere itself [**20**, p. 96].

We consider first a homogeneous Earth model, for which the variable of interest is the annual global mean surface temperature $T = T(t)$ (°C). The annual global mean insolation is given by the solar constant $Q = 343$ W/m^2. The incoming energy absorbed by the Earth is then modeled by the term $Q(1-\alpha)$, where α is the average global *albedo*, a measure of the extent to which the shortwave insolation is simply reflected back into space.

The loss of energy via OLR is modeled by a linear approximation $A + BT$, with parameters A (W/m^2) and B (W/(m^2 °C)) having been estimated from satellite measurements of OLR [**6**]. The actual physics of the atmosphere is a complicated combination of thermodynamics and radiative transfer; the reader is referred to the thorough introduction provided in [**15**].

A model equation for the global mean temperature is then given by

$$R\frac{dT}{dt} = Q(1-\alpha) - (A + BT). \tag{1}$$

The units on each side of equation (1) are W/m^2 or, equivalently, J/(s m^2). The quantity R is the heat capacity of the Earth's surface, with units J/(m^2 °C).

Equation (1) fits nicely into the sophomore-level ODE course. The reader is invited to show that, given any initial condition $(t_0, T(t_0))$, the corresponding solution converges to the equilibrium value $T^* = \frac{1}{B}(Q(1-\alpha) - A)$. We set $A = 202$ and $B = 1.9$, and we let $\alpha_w = 0.32$ and $\alpha_s = 0.62$ denote the albedo values for open water and snow covered ice, respectively [**21**]. For an ice free earth $\alpha = \alpha_w$, in which case a simple computation yields $T^* = 16.4$°C. If the Earth was covered by glaciers (the *snowball Earth* state), $\alpha = \alpha_s$, and T^* is a rather frosty -37.7°C.

Over time, glaciers may retreat due to summer melting if the annual global mean temperature is 0°C. The *critical temperature* at which one assumes glaciers are formed is typically taken to be $T_c = -10$°C. Given the parameter values above we see that, were the earth ever

in an ice free state, no glaciers would form per this model. Similarly, if the Earth were ever in a snowball state no ice would melt, with the planet remaining in a snowball state for all time. Observing that we currently have glaciers which do not cover the entire globe, one would thus conclude that the Earth has never been in either the ice free or snowball state. This evidently contradicts the environment of, say, the early Eocene (∼50 million years ago (Mya)), when temperatures were so warm alligators could be found above the article circle [**9**]. It may also contradict the extreme glacial episodes of the Neoproterozoic Era, roughly 700 Mya, about which we will have more to say below.

A 1-dimensional energy balance model

In seminal 1969 papers, M. Budyko [**3**] and W. Sellers [**17**] independently introduced EBM in which the surface temperature depends on both latitude and time. In each model the temperature is assumed to be constant on a given latitude circle. With θ denoting latitude, the use of the variable $y = \sin\theta$ turns out to be convenient in the model analysis. It is a nice exercise to show, for example, that y represents the proportion of the Earth's surface between latitudes $\arcsin(-y)$ and $\arcsin(y)$. We will refer to the "latitude" y in all that follows, trusting no confusion will arise on the reader's part.

The Budyko-Sellers model assumes the temperature distribution $T = T(t, y)$ is symmetric across the equator. It thus suffices to consider $y \in [0, 1]$, with $y = 0$ representing the equator and $y = 1$ corresponding to the north pole. Another nice exercise entails showing that the global annual average temperature is given simply by

$$\overline{T} = \int_0^1 T(t, y)dy. \tag{2}$$

Glaciers are incorporated into this model, with a corresponding adjustment to the albedo function. To that end, assume ice exists at every latitude above a given latitude $y = \eta$, while no ice exists at latitudes below η. We refer to η as the *ice line*, with the albedo now a function $\alpha_\eta(y) = \alpha(y, \eta)$ depending on y and the position of the ice line. As ice is more reflective than water or land, the albedo function will naturally be larger for latitudes above the ice line.

A second adjustment to equation (1) concerns the distribution of insolation as a function of latitude. The tropics receive more energy from the sun than do the polar regions on an annual basis, for example. This is taken into account by modeling the energy absorbed by the surface via the term

$$Qs(y)(1 - \alpha(y, \eta)),$$

where $s(y)$ represents the distribution of insolation over latitude, normalized so that

$$\int_0^1 s(y)dy = 1. \tag{3}$$

While $s(y)$ can be computed explicitly from first (astronomical) principles [**11**], it is uniformly approximated to within 2% by the polynomial $s(y) = 1.241 - 0.723y^2$ [**14**]. We use $s(y) = 1.241 - 0.723y^2$ in all that follows.

A final model adjustment concerns *meridional heat transport*, encompassing physical processes such as the heat flux carried by the circulation of the ocean and the fluxes of water vapor and heat transported via atmospheric currents. We focus henceforth on Budyko's model, in which the meridional transport term is simply $C(T - \overline{T})$, with $\overline{T}$ as in equation (2) and C (W/m^2 °C) a positive constant. Budyko's model equation is then

$$R\frac{\partial T}{\partial t} = Qs(y)(1 - \alpha(y, \eta)) - (A + BT) - C(T - \overline{T}). \tag{4}$$

Note the final term in equation (4) models the simple idea that warm latitudes (relative to the global mean temperature) lose heat energy through transport, while cooler latitudes gain heat energy.

It may appear at first glance that equation (4) is in spirit an ODE, given the lack of any $\frac{\partial T}{\partial y}$-terms. Note, however, that T must be known in particular as a function of y on the interval $[0, 1]$ in order to compute $\overline{T}$. As solutions to equation (4) live in an infinite dimensional function space, this model is not appropriate for that first differential equations course. As we'll see, however, the analysis of equation (4) would fit nicely in a mathematical modeling course having an emphasis on computation.

Equilibrium solutions

We begin this section by noting that the trail of formulae below is in fact relatively easy to deduce, with nothing more than algebra and calculus doing any heavy lifting.

An equilibrium solution $T^* = T^*(y, \eta)$ of equation (4) satisfies

$$Qs(y)(1 - \alpha(y, \eta)) - (A + BT^*) - C(T^* - \overline{T^*}) = 0. \tag{5}$$

Integration of each side of equation (5) with respect to y from 0 to 1, while recalling equation (3), yields

$$Q(1 - \overline{\alpha}(\eta)) - (A + B\overline{T^*}) = 0, \quad \text{where } \overline{\alpha}(\eta) = \int_0^1 s(y)\alpha(y, \eta)dy. \tag{6}$$

Solving for $\overline{T^*}$, we then have the global mean temperature at equilibrium is given by

$$\overline{T^*} = \overline{T^*}(\eta) = \frac{1}{B}(Q(1 - \overline{\alpha}(\eta)) - A). \tag{7}$$

Now plugging $\overline{T^*}$ from equation (7) into equation (5), and solving the resulting equation for

T^*, we obtain

$$\begin{aligned} T^* = T^*(y,\eta) &= \frac{1}{B+C}\left(Qs(y)(1-\alpha(y,\eta)) - A + C\overline{T^*}\right) \\ &= \frac{Q}{B+C}\left(s(y)(1-\alpha(y,\eta)) + \frac{C}{B}(1-\overline{\alpha}(\eta))\right) - \frac{A}{B}, \end{aligned} \tag{8}$$

with $\overline{\alpha}(\eta)$ as in equation (6). Given that we assume $s(y)$ and each of A, B, C and Q are known, we see T^* (and hence $\overline{T^*}$) depends on the albedo function $\alpha(y,\eta)$ and, in particular, on the position η of the ice line.

Following Budyko, we first consider the 2-step albedo function

$$\alpha(y,\eta) = \begin{cases} \alpha_w, & y < \eta \\ \alpha_s, & y > \eta, \end{cases} \qquad \alpha_w = 0.32,\ \alpha_s = 0.62. \tag{9}$$

With a goal of finding T^*, $\overline{\alpha}(\eta)$ is easily computed in this case:

$$\overline{\alpha}(\eta) = \int_0^\eta \alpha_w s(y)dy + \int_\eta^1 \alpha_s s(y)dy = \alpha_s - (\alpha_s - \alpha_w)(1.241\eta - 0.241\eta^3).$$

We can now use equation (8) to plot several equilibrium temperature profiles, as in Figure 1. For $\eta \in (0,1)$ each of these profiles has a discontinuity at η due to our choice of $\alpha(y,\eta)$.

In the ice free state $\alpha = \alpha_w$ for all y, and we see from Figure 1 that the equilibrium temperature exceeds T_c at all latitudes y in this case. Hence if the parameter values remain fixed the planet never exits an ice free state, as with the homogeneous Earth model. Similarly, $\alpha = \alpha_s$ for all y in the snowball state, and the equilibrium temperature at all latitudes y is less than T_c. Thus if the Earth becomes completely ice covered it once again remains so for all time.

Each specification of an ice line η yields an equilibrium temperature profile via equation (8). Put another way, there are infinitely many equilibrium functions, one for each $\eta \in [0,1]$. What happens if we add the constraint that the temperature at the ice line at equilibrium must equal $T_c = -10°\text{C}$?

It is natural to define the temperature $T^*(\eta,\eta)$ at the ice line at equilibrium by the average

$$h(\eta) = T^*(\eta,\eta) = \frac{1}{2}\left(\lim_{y\to\eta^-} T^*(y,\eta) + \lim_{y\to\eta^+} T^*(y,\eta)\right).$$

We use the notation $h(\eta)$ to emphasize that this average is a function of the single variable η.

Using the continuity of $s(y)$, along with equations (8) and (9), a computation reveals

$$\begin{aligned} h(\eta) &= \frac{1}{B+C}\left(Qs(\eta)(1-\alpha_0) - A + C\overline{T^*}\right), \\ &= \frac{Q}{B+C}\left(s(\eta)(1-\alpha_0) + \frac{C}{B}(1-\overline{\alpha}(\eta))\right) - \frac{A}{B}, \quad \alpha_0 = \frac{1}{2}(\alpha_w + \alpha_s). \end{aligned} \tag{10}$$

The plot of the function $h(\eta)$ in Figure 2 discloses the existence of two ice line positions $\eta_1, \eta_2 \in (0,1)$, with $\eta_1 < \eta_2$ and $h(\eta_1) = -10°\text{C} = h(\eta_2)$. The corresponding equilibrium functions are also plotted in Figure 2. Note that $T^*(y, \eta_1)$ corresponds to a very large ice cap, with mean global annual temperature a frigid $\overline{T^*}(\eta_1) = -21.4°\text{C}$. The ice cap for $T^*(y, \eta_2)$ is closer to that which we experience today, with $\overline{T^*}(\eta_2) = 14.9°\text{C}$, a much more pleasant climate! We will have more to say about these two equilibrium solutions, distinguished by $h(\eta_i) = -10°\text{C}$, $i = 1, 2$, shortly.

A bifurcation diagram

Equation (4) is teeming with parameters. In dynamical systems one is often interested in studying the ways in which solutions change as one or more parameters are varied. At this point we might investigate, for example, how the position η of the ice line at equilibrium changes as a parameter is varied. While Budyko focused on the change in η at equilibrium as a function of Q (the solar "constant" varies significantly over long time scales), we choose to keep all parameters fixed with the exception of A.

Recall that A is the constant in the term modeling OLR in equation (4). Carbon dioxide in our atmosphere interacts with radiation emitted by the Earth, strongly absorbing OLR in a range of spectral wavelengths [**15**, chapter 4]. One can thus think of A as a proxy for the amount of CO_2 in the atmosphere: An increase in CO_2 results in a decrease in OLR, which can be modeled by a decrease in A. Similarly, a decrease in atmospheric CO_2 results in an increase in OLR, and hence an increase in A.

A correspondence between the position η of the ice line at equilibrium and the parameter A can be realized by setting $h(\eta)$ from equation (10) equal to -10°C and solving for A. After a bit of algebra, one arrives at

$$A(\eta) = \frac{B}{B+C}\left(Qs(\eta)(1-\alpha_0) + \frac{C}{B}Q(1-\overline{\alpha}(\eta)) + 10(B+C)\right). \tag{11}$$

We use equation (11) to generate the bifurcation diagram shown in Figure 3. The horizontal line drawn at $\eta = 1$ in Figure 3 corresponds to an ice free planet, which occurs if the amount of CO_2 in the atmosphere is sufficiently large. In this scenario OLR is trapped by the atmosphere to a great extent, leading to higher surface temperatures (the "greenhouse effect" [**15**, chapter 3]). Similarly, the line drawn at $\eta = 0$ corresponds to the snowball Earth state, which occurs for sufficiently low CO_2 values. The dotted vertical line in Figure 3 represents $A = 202$, for which the values $\eta_1 < \eta_2$, discussed previously and illustrated in Figure 2, satisfy $h(\eta_1) = -10°\text{C} = h(\eta_2)$.

Note the lack of any equilibrium solutions with $h(\eta) = -10°\text{C}$ if $A > A_0 = 211.641$, while two such equilibrium solutions exist if A is slightly less than A_0. (A_0 is determined by maximizing $A(\eta)$ on $(0,1)$.) We say a *bifurcation* occurs at $A = A_0$, which is often called

a *tipping point* in the climate science literature. If the amount of CO_2 in the atmosphere decreases in such a way that A increases through A_0, runaway cooling occurs and the climate plunges into the snowball Earth state. This serves to illustrate the positive *ice albedo feedback*, which works as follows. Suppose that A begins to increase away from $A = A_0$. As more OLR escapes to space the planet cools down and the ice line descends toward the equator. As more of the surface is now covered in ice, the planetary albedo increases, leading to lower temperatures and further movement of the ice line toward the equator.

From both dynamical systems and modeling perspectives, the bifurcation diagram discussed above comes with one major caveat: There is as yet no mechanism through which one can determine the *stability* of equilibrium solutions $T^*(y, \eta)$. That is, there is an implicit assumption in previous interpretations of Budyko's model that the long term behavior of solutions to equation (4) is determined by the equilibrium solutions.

A simple example that this need not be the case is provided by the damped pendulum, for which both the inverted and straight downward positions represent equilibrium solutions. The former is an unstable equilibrium in that solutions starting in a nearly vertical position move away from the vertical when released. The latter is an attracting equilibrium as solutions which start from a nearly downward position approach the downward equilibrium solution over time. The unstable equilibrium plays no (or, at best, very little) role in determining the dynamics of the model.

Budyko and several subsequent authors did investigate stability issues related to the position of η at equilibrium as a function of a parameter (typically Q; see [**4**], for example). This again begs the mathematical question, however, of whether solutions to equation (4) approach $T^*(y, \eta)$ for given, fixed parameter values.

The stability type of equilibrium solutions $T^*(y, \eta)$ has been rigorously established only recently [**23**]; we turn now to this result, along with the requisite model enhancement.

The Budyko-Widiasih model

The result of an insightful computational experiment is presented in Figure 4. Start by selecting a specific η value and an initial temperature profile $T_0(y, \eta)$; for example, $\eta = 0.2$ and a balmy $T_0(y, \eta) = 39 - 10y^2$. In essence, we approximate the evolution of T_0 under equation (4) via Euler's method, generating a sequence of temperature profiles $\{T_n\}$. The plot in Figure 4 indicates that $T_n \to T^*(y, 0.2)$ over time, where $T^*(y, 0.2)$ is the equilibrium temperature function corresponding to $\eta = 0.2$. We thus have numerical evidence of the attractive nature of $T^*(y, 0.2)$ in some infinite dimensional function space.

Observe also that the ice line remains stationary as the planet cools from the initial, warmer $T_0(y, \eta)$ down to $T^*(y, 0.2)$. It is reasonable to expect the ice line to move equator-

ward as the temperature decreases.

In a natural enhancement of Budyko's model, E. Widiasih [**23**] added a second equation to equation (4) to account for the dynamics of the ice line, yielding the system

$$\begin{aligned} R\frac{\partial T}{\partial t} &= Qs(y)(1-\alpha(y,\eta)) - (A+BT) - C(T-\overline{T}) \\ \frac{d\eta}{dt} &= \epsilon(T(\eta,\eta) - T_c). \end{aligned} \tag{12}$$

Given a temperature profile $T(y,\eta)$, one checks the temperature $T(\eta,\eta)$ at the ice line. If $T(\eta,\eta)$ is less than T_c, ice forms and the ice line descends, while the ice line moves poleward if $T(\eta,\eta) > T_c$. Motivated by paleoclimate data, McGehee and Widiasih [**12**] have proposed a value for ϵ on the order of 10^{-13}. The size of ϵ reflects the fact that the ice sheets move very slowly in response to changes in temperature.

Equilibrium solutions for system (12) consist of pairs $(T^*(y,\eta),\eta)$ for which $T^*(y,\eta)$ satisfies both equation (4) and $T^*(\eta,\eta) = -10°\text{C}$. Recall, for example, there are precisely two such solutions for A between roughly $A = 199$ and $A = 211$, as indicated in Figure 3.

In a tour de force, Widiasih proved the existence of an attracting one-dimensional curve, consisting of temperature profile–ice line position pairs, which is invariant under system (12). Moreover, she proved the dynamics on this curve is described by the relatively simple ODE

$$\frac{d\eta}{dt} = \epsilon(h(\eta) - T_c), \tag{13}$$

with $h(\eta)$ as in equation (10). Despite the comparatively unruly nature of the function $h(\eta)$, equation (13) can be analyzed by students in the first ODE course with the aid of technology simply by sketching and interpreting the graph of $h(\eta)$ (as in Figure 2).

Indeed, coupling Widiasih's result with the plot of $h(\eta)$ in Figure 2, we have the following lovely conclusions. If $\eta \in (\eta_2, 1),\ h(\eta) < -10°\text{C}$ implies ice will form and the ice line will descend. For $\eta \in (\eta_1, \eta_2),\ h(\eta) > -10°\text{C}$ and the ice line moves poleward as the ice melts. We conclude that η_2 corresponds to an attracting equilibrium solution of system (12). In addition, $h(\eta) < -10°\text{C}$ for $\eta \in (0, \eta_1)$, forcing the ice line to move equatorward for these latitudes, and we see that η_1 corresponds to an unstable rest point. Hence the small ice cap is a stable solution, while the large ice cap is unstable.

The inclusion of an equation for movement of the ice line places the Budyko-Widiasih model on solid ground from a dynamical systems point of view. One can now incorporate model dynamics in redrawing the bifurcation diagram originally presented in Figure 3. This dynamic bifurcation diagram (Figure 5) is of the type discussed in introductory differential equations texts such as [**2**].

The reader will perhaps have noted that system (12) admits a boundary given by $\eta = 0$ (the equator) and $\eta = 1$ (the north pole). Widiasih succeeded in incorporating these two η values in her reduction to equation (13), concluding that the ice free state is unstable,

while the snowball Earth state is stable. This follows in essence from Figure 2 by observing $h(1) < -10°\text{C}$ and $h(0) < -10°\text{C}$ (see [**23**] for details).

A second remark concerns the 2-step albedo function $\alpha(y, \eta)$, which in Widiasih's theorem is in fact assumed to be continuous. A typical continuous approximation to the albedo function given in equation (9) is

$$\alpha(y, \eta) = \frac{1}{2}(\alpha_s + \alpha_w) + \frac{1}{2}(\alpha_s - \alpha_w) \tanh M(y - \eta), \tag{14}$$

where M is a parameter controlling the sharpness of the transition from open water to ice (see Figure 6). The equilibrium temperature profiles $T^*(y, \eta)$ are now continuous at η when using albedo function (14), while the qualitative nature of the graph of $h(\eta)$ in Figure 2 remains the same [**23**]. In particular, the model still results in a small stable ice cap and a large unstable ice cap. The use of equation (14) does force one to use technology to sketch equilibrium solutions and bifurcation diagrams, however, as $\overline{\alpha}(\eta)$ becomes more of a challenge to compute.

The behavior of solutions to system (12) is intimately connected to the qualitative nature of the albedo function. We have seen that an albedo function $\alpha(y, \eta)$ with essentially one value south of the ice line and one larger value north of the ice line leads to two equilibria, one attracting and the other unstable. Might the Budyko-Widiasih model, with an appropriate adjustment to $\alpha(y, \eta)$, be capable of modeling the great glacial episodes of the Neoproterozoic Era?

Extreme glacial events of the past

Typing "snowball Earth" into one's preferred search engine and hitting *enter* results in a cornucopia of information (the interested reader might start at [**18**]). Indeed, a wealth of geological and geochemical evidence exists indicating that ice sheets flowed into the ocean near the equator during two Neoproterozoic glacial periods, roughly 630 Mya and 715 Mya ([**8**], [**1**], [**16**] and references within each).

There are many on each side of the snowball Earth fence, some supporting its occurrence, while others believe the descent of the glaciers halted prior to reaching the equator. There is evidence, for example, suggesting that photosynthetic eukaryotes, and perhaps certain types of sponges, thrived both before and in the aftermath of these glacial episodes. This in turn lead to the proposal of the *Jormungand* global climate state [**1**], an alternative to the snowball Earth hypothesis. In the Jormungand climate the glaciers descend to tropical latitudes without triggering a runaway snowball Earth event. In this way sunlight can reach organisms in the ocean in a band of open water about the equator.

One obvious difficulty, successfully modeled in [**1**] through atmospheric dynamics considerations, centers on specifying a mechanism by which the planet can cool to the extent

glaciers exist in the tropics, while avoiding complete planetary glaciation. A second question of interest, resolved in [**22**], is whether a dynamically stable Jormungand state can be realized in the Budyko-Widiasih model through an adjustment in the albedo function first suggested in [**1**].

The Jormungand model

Sea ice will be covered with snow only if there is sufficient precipitation. Using the albedo effect of clouds in the atmosphere above the tropics, as well as the role of Hadley cells in atmospheric circulation, an argument is made in [**1**] for net evaporation in a tropical latitude band during the cold climate of the Neoproterozoic glacial periods. It would then follow that new sea ice forming in this band would fail to acquire a snow cover due to insufficient precipitation, relative to evaporation. Bare sea ice has an albedo greater than that of open water, and less than that of snow covered ice. In particular, as bare sea ice absorbs more insolation than does snow covered ice, the existence of this band is a candidate for the mechanism by which the advance of the glaciers might halt prior to reaching the equator.

It is natural to include a bare sea ice albedo α_i, with $\alpha_w < \alpha_i < \alpha_s$, in the albedo function for the Jormungand climate model. The ice line η will continue to be regarded as the boundary between open water and (in this case bare) sea ice. As in [**1**], we assume no bare sea ice exists above $y = 0.35$. Thus for $\eta \geq 0.35$ there is only open water and snow covered sea ice, as before. The albedo function α_J has three "steps," however, corresponding to α_w, α_i and α_s, for $\eta < 0.35$. Looking to apply Widiasih's theorem, we supply such a continuous albedo function $\alpha_J(y, \eta)$ in Figure 6. This function is designed so that the extent of the bare sea ice decreases linearly from 0.35 when $\eta = 0$ to zero when $\eta \geq 0.35$. A snowball earth, for example, now has bare sea ice extending from the equator to latitude $y = 0.35$, and snow covered ice north of $y = 0.35$. A formula for such an α_J is provided in [**22**].

The use of α_J in system (12) requires the new computation

$$\overline{\alpha_J}(\eta) = \int_0^1 \alpha_J(y, \eta) s(y) dy$$

in the analysis. This can be accomplished via *Mathematica* or *Matlab*, with a few of the resulting equilibrium temperature profiles $T_J^*(y, \eta)$ of equation (4) sketched in Figure 7. One can apply Widiasih's theorem to reduce system (12) to the study of the analog of equation (13), one with $h(\eta)$ replaced by

$$h_J(\eta) = \frac{Q}{B + C} \left(s(\eta)(1 - \alpha_J(\eta, \eta)) + \frac{C}{B}(1 - \overline{\alpha_J}(\eta)) \right) - \frac{A}{B}, \tag{15}$$

for the Jormungand model [**22**]. One can then numerically compute and graph the function $h_J(\eta)$ as in Figure 8.

Parameter values appropriate to the Neoproterozoic Era are difficult to specify. It is known that the solar constant Q was 94% of its current value 700 Mya. As in [**1**], we assume meridional heat transport was less efficient due to the very cold climate, thereby reducing the value of parameter C. Moreover, due the massive ice sheets, the draw down of CO_2 from the atmosphere via silicate weathering [**15**] was reduced, potentially leading to smaller values of A and B. Albedo values for the various surface components are difficult to specify as well. Admittedly then, and following the lead of the authors of [**1**], we fiddled with the parameters a bit to get what we were looking for.

The plot in Figure 8 indicates there are three equilibrium solutions, with ice lines $n_1 < \eta_2 < \eta_3$ satisfying $h_J(\eta_i) = -10°\text{C}$, $i = 1, 2, 3$. As in the previous analysis, η_3 corresponds to a small stable (attracting) ice cap, while η_2 is unstable. However, as $h_J(\eta)$ is greater than $-10°\text{C}$ on $(0, \eta_1)$, ice melts in this region and the ice line moves toward η_1. As $h_J(\eta)$ is less than $-10°\text{C}$ on (η_1, η_2), ice forms in this region, and again the ice line moves toward η_1. We conclude that η_1 corresponds to an attracting equilibrium solution of system (12), one with an ice line in tropical latitudes. In addition, while the ice free state is once again unstable ($h_J(1) < -10°\text{C}$), the snowball Earth state becomes unstable ($h_J(0) > -10°\text{C}$) in the Budyko-Widiasih rendering of the Jormungand model.

A dynamically resolved bifurcation diagram for the Jormungand model is presented in Figure 9. The phase line at $A = 180$ in Figure 9 corresponds the the graph of $h_J(\eta)$ plotted in Figure 8. For a range of A values (roughly between 176.5 and 182), system (12) admits both small and large stable ice caps, with an intermediate unstable ice cap. As A increases through roughly $A = 182$ (so that atmospheric CO_2 decreases), the small equilibrium ice cap disappears and solutions now converge to an equilibrium having a large stable ice cap. A second tipping point occurs near $A = 191.5$ when the large ice cap vanishes, resulting in a runaway snowball Earth event.

A final bifurcation occurs when A decreases through $A = 169$, at which point the large ice cap disappears and the system heads toward the ice free state. We see that a simple adjustment to the albedo function (one allowing, however, for the application of Widiasih's theorem), has lead to a remarkable change in the behavior of the energy balance model.

Conclusion

The study of climate presents enormous challenges in efforts to better understand the interactions and influences of its numerous components. Energy balance models lie on the conceptual, or low order, end of the modeling spectrum, with a focus placed on the major elements of climate systems. It is decidedly not the role of EBM to provide detailed predictions of climate, even on a planetary scale. One aspect of the utility of EBM, as illustrated in this article, is the way in which such models can provide a broad view of the important role

played by crucial climate components. Based on the Budyko-Sellers and Budyko-Widiasih models, for example, we have gained insight here into the sensitivity of climate to changes in albedo.

Widiasih's theorem provides an answer as to the stability type of equilibrium solutions of the Budyko-Sellers EBM. As this theorem requires continuous versions of model-appropriate albedo functions (recall equation (14)), a student encountering this material in a mathematical modeling course would need technology to compute equilibrium temperature profiles, bifurcation diagrams, and to investigate model sensitivity to changes in parameters. There is a wealth of material in climate modeling at the level of EBM appropriate for students in such a computational modeling course.

The interaction of science and mathematics in the study of climate is also noteworthy. The physics of blackbody radiation, the chemistry involved in untangling what is meant by the "greenhouse effect," the intricate role played by the carbon cycle in the evolution of climate—there is an inherent cross-disciplinary appeal to this material. From mathematical and computational modeling perspectives, the study of energy balance models is rife with possibilities for exploration at the undergraduate level.

References

1. D. Abbot, A. Viogt and D. Koll, The Jormungand global climate state and implications for Neoproterozoic glaciations, *J. Geophys. Res.* **116** (2011) (D18103) doi:10.1029/2011JD015927.
2. P. Blanchard, R. Devaney and G.R. Hall, *Differential Equations*, 3rd ed., Thomson Brooks/Cole, Belmont CA, 2006.
3. M.I. Budyko, The effect of solar radiation variation on the climate of the Earth, *Tellus* **5** (1969) 611–619.
4. R. Cahalan and G. North, A stability theorem for energy-balance climate modes, *J. Atmos. Sci.* **36** (1979) 1178-1188.
5. Community Earth System Model, National Center for Atmospheric Research; see `http://www.cesm.ucar.edu/`.
6. C. Graves, W-H. Lee and G. North, New parameterizations and sensitivities for simple climate models, *J. Geophys. Res.* **198** (D3) (1993) 5025–5036.
7. F. Guterl, Searching for clues to calamity, *New York Times*, July 21, 2012, A19.
8. P. Hoffman and D. Schrag, The snowball Earth hypothesis: testing the limits of global change, *Terra Nova* **14** (3) (2002) 129-155.
9. P. Jardine, Patterns in palaeontology: the Paleocene–Eocene thermal maximum, *Paleontology [online]* **1** (5) (2011) 2-7; available at `http://www.palaeontologyonline.com/articles/2011/the-paleocene-eocene-thermal-maximum/`.

10. Mathematics and Climate Research Network; see http://www.mathclimate.org/.

11. R. McGehee and C. Lehman, A paleoclimate model of ice-albedo feedback forced by variations in Earth's orbit, *SIAM J. Appl. Dyn. Syst.* **11** (2) (2012) 684-707.

12. R. McGehee and E. Widiasih, A finite dimensional version of a dynamic ice-albedo feedback model, preprint.

13. G. North, Analytical solution to a simple climate model with diffusive heat transport, *J. Atmos. Sci.* **32** (1) (1975) 1301-1307.

14. G. North, Theory of energy-balance climate models, *J. Atmos. Sci.* **32** (11) (1975) 2033–2043.

15. R. Pierrehumbert, *Principles of Planetary Climate*, Cambridge University Press, New York NY, 2010.

16. R. Pierrehumbert, D. Abbot, A. Voigt and D. Koll, Climate of the Neoproterozoic, *Annu. Rev. Earth Planet. Sci.* **39** (May 2011) 417-460.

17. W. Sellers, A global climatic model based on the energy balance of the Earth-Atmosphere system, *J. Appl. Meteor.* **8** (1969) 392–400.

18. Snowball Earth; see http://www.snowballearth.org/.

19. Society for Industrial and Applied Mathematics Conference on Applications of Dynamical Systems, Snowbird UT, May 2011; see http://www.siam.org/meetings/ds11/index.php.

20. S. Solomon, D. Qin, M. Manning, Z. Chen, M. Marquis, K.B. Averyt, M. Tignor and H.L. Miller (eds.), *Contribution of Working Group I to the Fourth Assessment Report of the Intergovernmental Panel on Climate Change, 2007*, Cambridge University Press, Cambridge UK and New York NY; available at http://www.ipcc.ch/publications_and_data/publications_and_data_reports.shtml#.UC0BskSGKOX.

21. K.K. Tung, *Topics in Mathematical Modeling,* Princeton University Press, Princeton New Jersey, 2007.

22. J.A. Walsh and E. Widiasih, A dynamics approach to low order climate models, preprint.

23. E. Widiasih, Dynamics of Budyko's energy balance model, preprint.

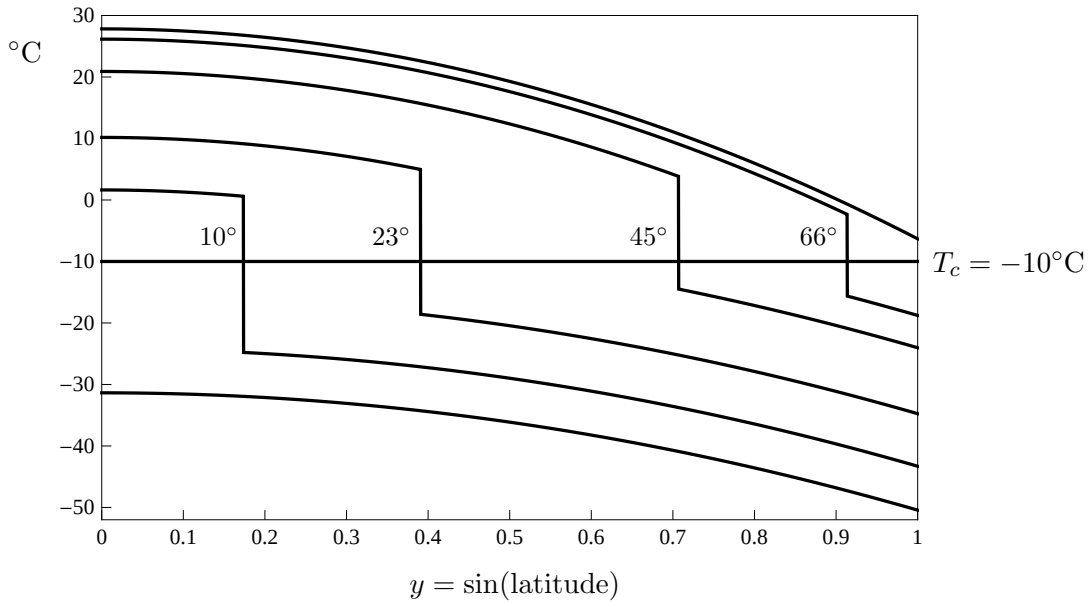

Figure 1. Equilibrium temperature profiles $T^*(y, \eta)$ with albedo $\alpha(y, \eta)$ as in equation (9). The bottom profile is for the snowball Earth state, while the top curve is for the ice free state. Parameters: $A = 202, B = 1.9, C = 3.04, Q = 343, \alpha_w = 0.32, \alpha_s = 0.62$.

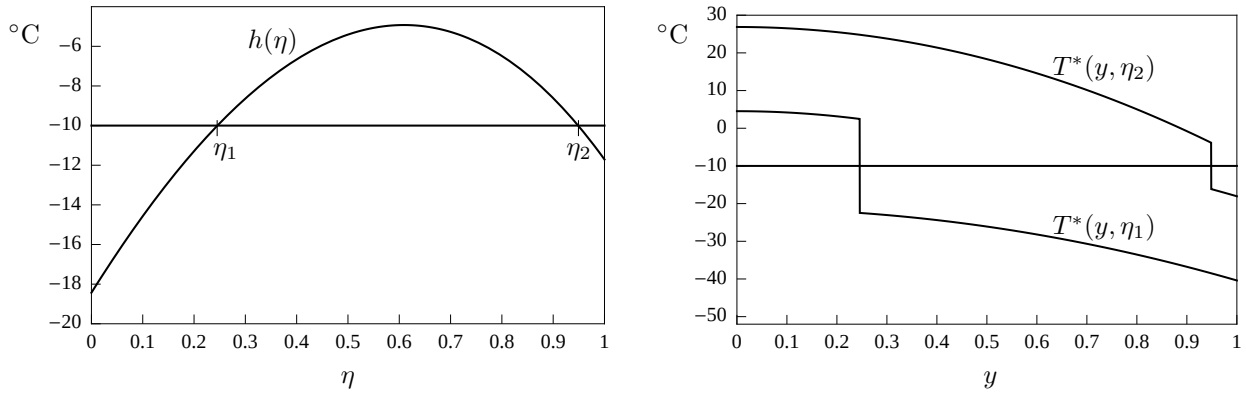

Figure 2. *Left.* Two ice line latitudes satisfying $h(\eta) = -10°\text{C}$. *Right.* The corresponding equilibrium temperature profiles. Parameters as in Figure 1.

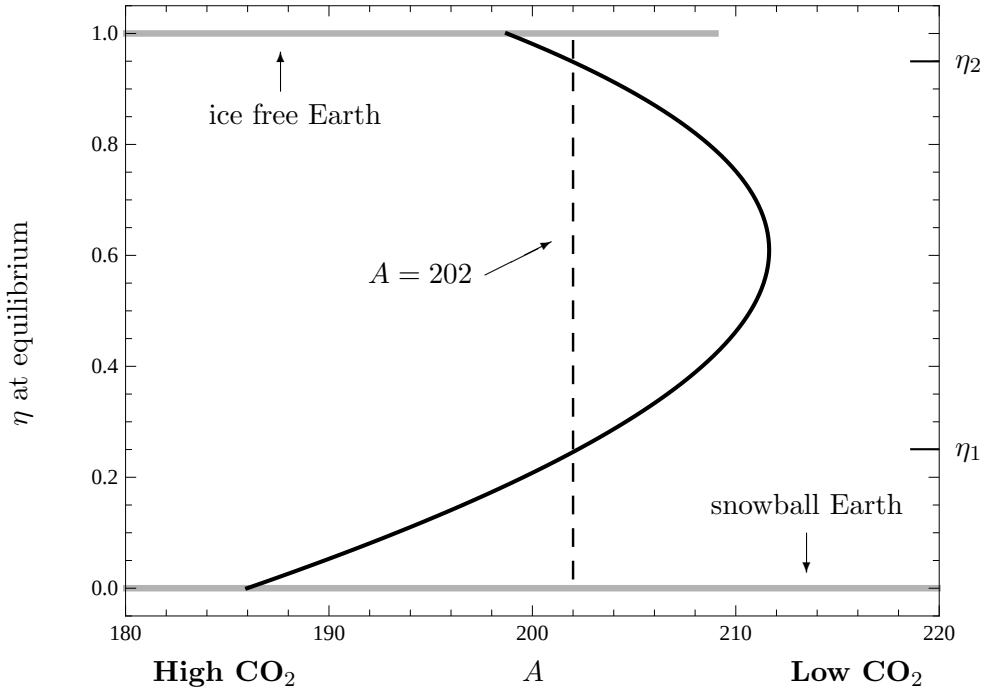

Figure 3. The position of the ice line η, satisfying $h(\eta) = -10°\text{C}$ at equilibrium, as the parameter A varies. Remaining parameter values as in Figure 1.

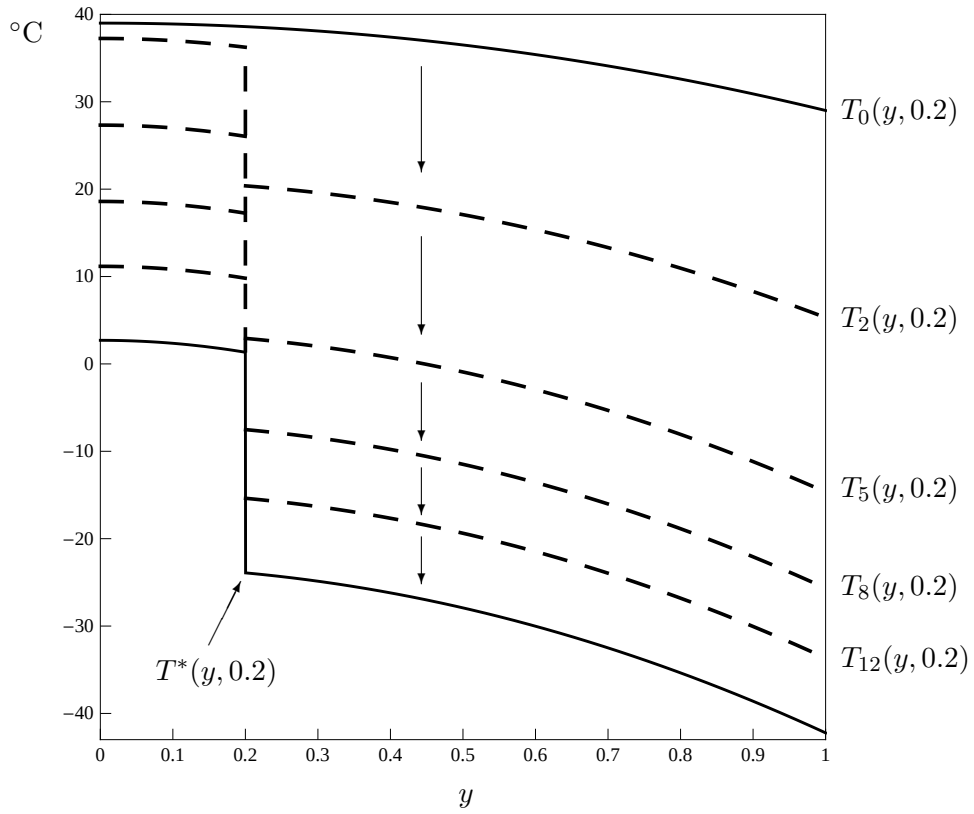

Figure 4. Euler's Method applied to equation (4) with initial profile a very warm $T_0(y, 0.2) = 39 - 10y^2$. It appears $T_n(y, 0.2) \to T^*(y, 0.2)$ as $n \to \infty$.

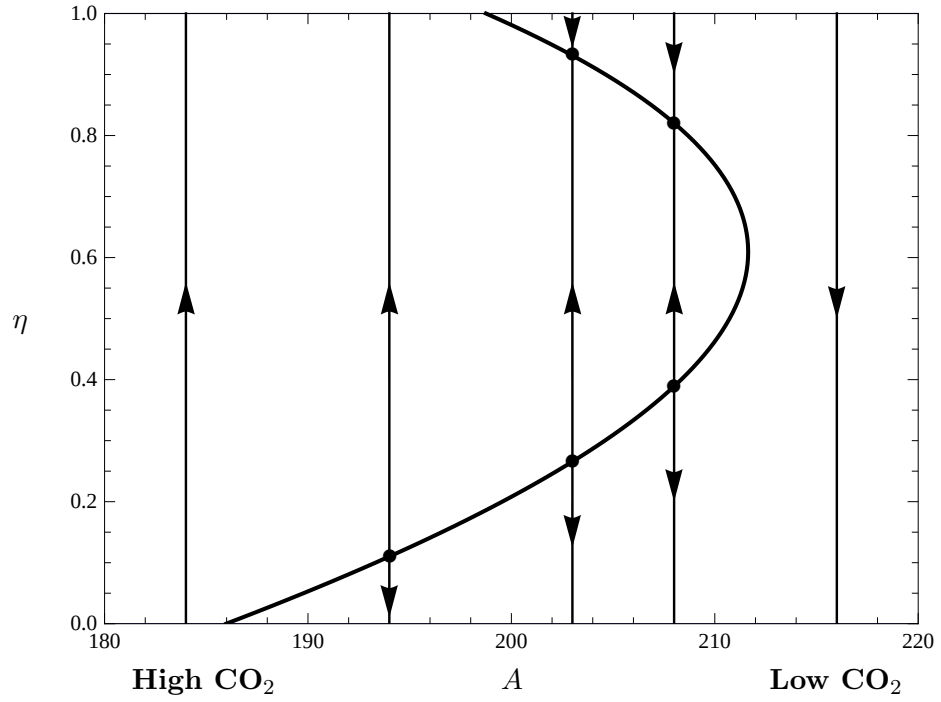

Figure 5. The dynamic bifurcation diagram for the Budyko-Widiasih model. Arrows indicate the movement of the ice line as solutions to system (12) evolve.

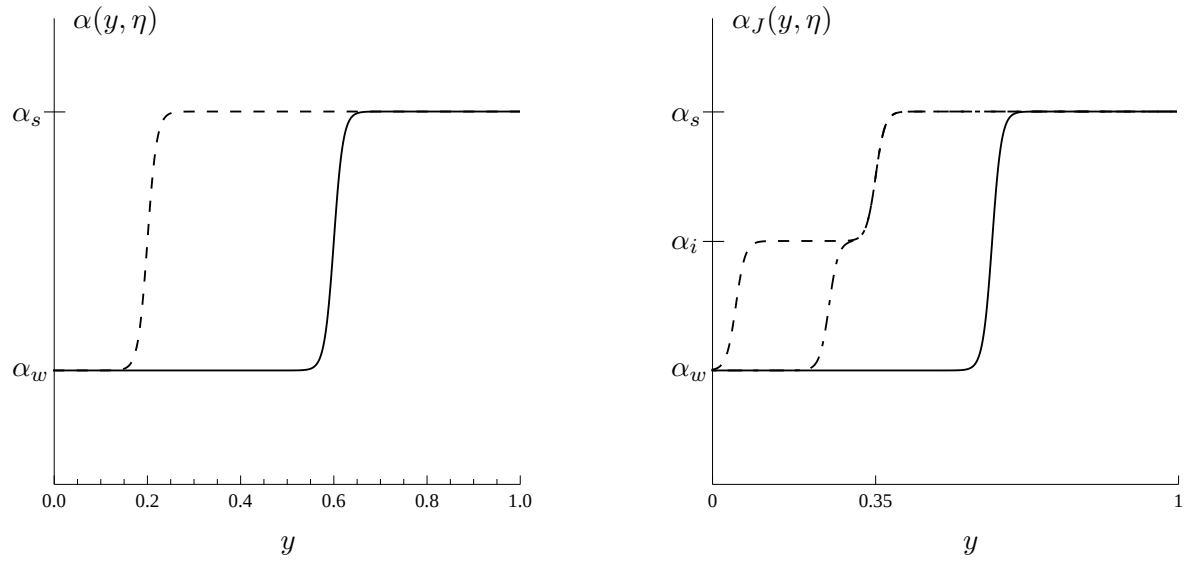

Figure 6. *Left.* The albedo function given in equation (14). Dashed: $\eta = 0.2$. Solid: $\eta = 0.6$. *Right.* The albedo function $\alpha_J(y, \eta)$ for the Jormungand model. Dashed: $\eta = 0.05$. Dash-dot: $\eta = 0.25$. Solid: $\eta = 0.6$.

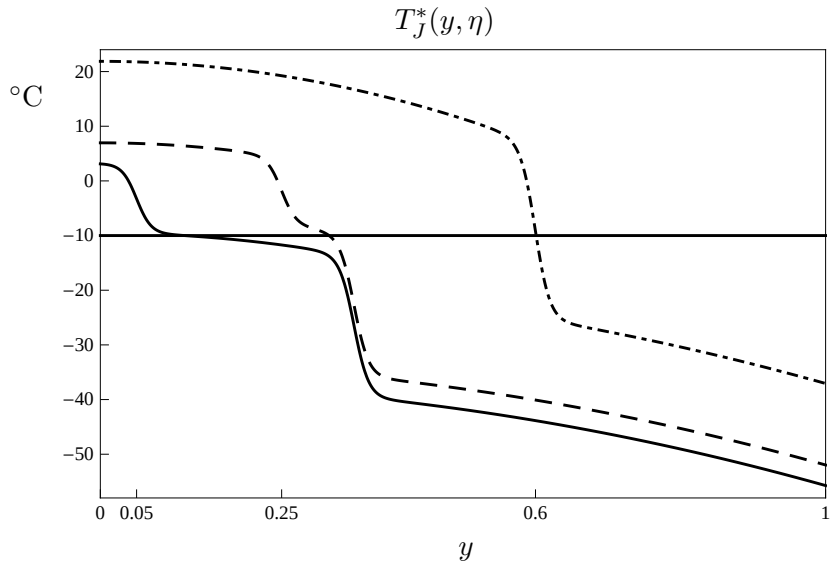

Figure 7. Equilibrium solutions $T_J^*(y,\eta)$ of equation (4) with the Jormungand model albedo function $\alpha_J(y,\eta)$ provided in Figure 6. Solid: $\eta = 0.05$. Dashed: $\eta = 0.25$. Dash-dot: $\eta = 0.6$.

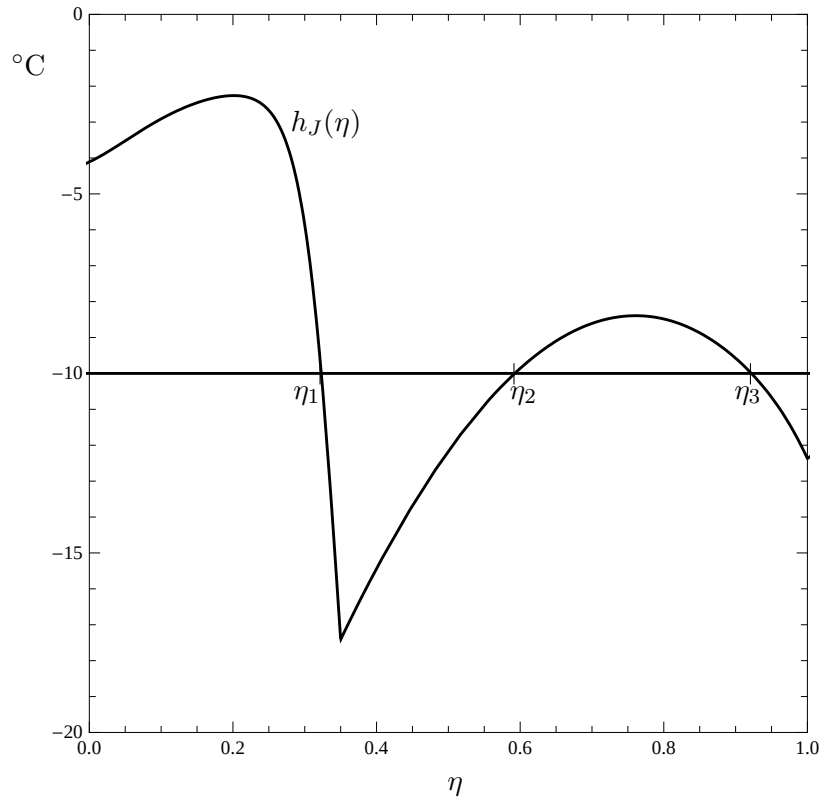

Figure 8. System (12) admits three equilibrium solutions with $h_J(\eta_i) = -10°\text{C}, \quad i = 1, 2, 3,$ in the Jormungand model with albedo function $\alpha_J(y, \eta)$ as provided in Figure 6. Parameters: $A = 180, B = 1.5, C = 2.25, Q = 321, \alpha_w = 0.32, \alpha_i = 0.44, \alpha_s = 0.74.$

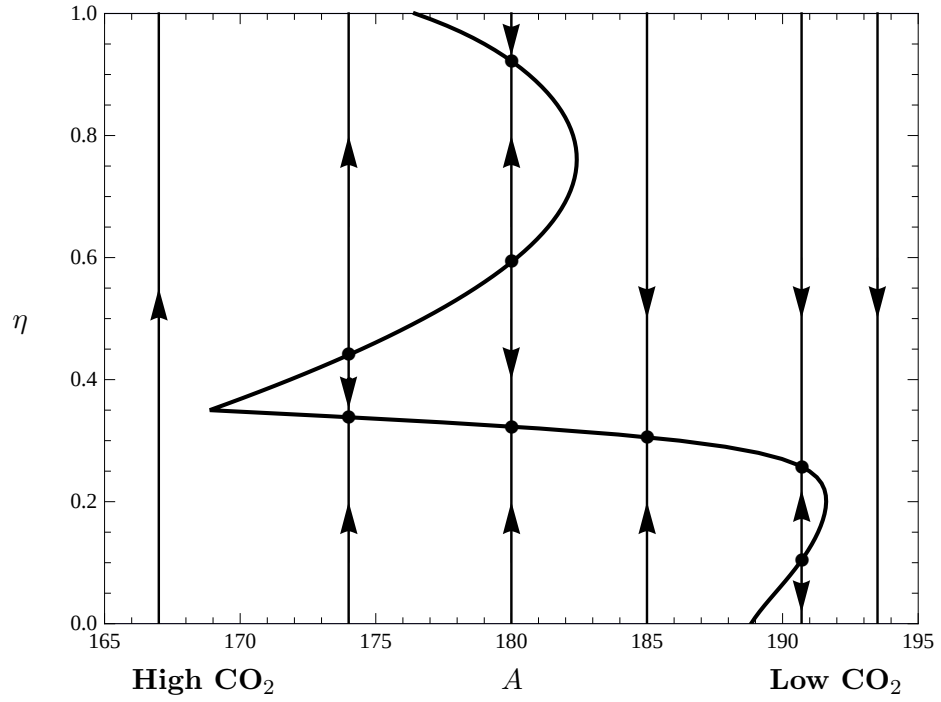

Figure 9. The dynamic bifurcation diagram for the Jormungand model. Arrows indicate the movement of the ice line as solutions to system (12) evolve, with albedo function $\alpha_J(y, \eta)$.